Swelling Behavior of Novel Protein-Based Superabsorbent Nanocomposite

G. Bagheri Marandi,[1] G. R. Mahdavinia,[2] Sh. Ghafary[1]

[1]*Department of Chemistry, Islamic Azad University, Karaj Branch, Karaj, Iran*
[2]*Department of Chemistry, Faculty of Science, University of Maragheh, Maragheheh, Iran*

Received 15 September 2009; accepted 26 June 2010
DOI 10.1002/app.33016
Published online 9 November 2010 in Wiley Online Library (wileyonlinelibrary.com).

ABSTRACT: A novel superabsorbent nanocomposite based on hydrolyzed collagen was synthesized by simultaneously graft copolymerization of 2-acrylamido-2-methylpropane sulfonic acid (AMPS) and acrylamide (AAm). Sodium montmorilonite (Na-MMt) was used as clay. Methylenebisacrylamide (MBA) and ammonium persulfate (APS) were used as crosslinker and initiator, respectively. The effect of reaction variables such as nanoclay content, MBA and APS concentrations as well as the AMPS/AAm weight ratio on the water absorbency of nanocomposites was investigated. Although the water absorbency was decreased by increasing of MBA concentration, an optimum swelling capacity was achieved for clay, APS, and AMPS/AAm variables. The structure of nanocomposite was identified using FTIR spectroscopy, XRD patterns, and scanning electron microscopy graphs. The effect of swelling media comprising various dissolved salts and different pHs was studied. Also, water retention capacity was studied, and the results showed that inclusion of Na-MMt nanoclay causes an increase in water retention under heating.
 J Appl Polym Sci 120: 1170–1179, 2011

Key words: nanocomposite; superabsorbent; collagen; swelling; pH-sensitive

INTRODUCTION

Hydrogels are three-dimensional hydrophilic networks that can absorb, swell, and retain aqueous fluids up to > 20 wt % times their dried weight.[1] Hydrogels with high swelling capacity are known as superabsorbents.[2] Because of their excellent response to changing environment conditions such as temperature,[3] pH,[4] and solvent composition,[5] hydrogels have been attracting many industrial applications.[6,7] Because of their water retention property and subsequently, the slow release of water from swollen hydrogels, hydrogels with high swelling capacity are of special interest as potential water retainer systems for agriculture fields. Also, in the field of agriculture, the slow release of water from the polymeric matrix opens another potential area of application that is related to load of agrochemicals into hydrogels. In swollen hydrogels containing agrochemicals, not only does water release takes place, but also the agrochemical will be released together with water.[8–11]

The higher production cost and low gel strength of these hydrogels, however, restrict their application widely. To improve these limitations, inorganic compounds with low cost can be used. The introduction of inorganic fillers to a polymer matrix increases its strength and stiffness properties.[12] Conventional hydrogel composites have been reported by scientists.[13–15] Inclusion of conventional microscale clays into hydrogels produces aggregated and agglomerated points. This is attributed to the heterogeneous dispersion of clay particles.[16] It has been reported that the type of dispersion of clay in composites determines the properties of polymer composites.[17] In addition to aggregated clay–polymer composites, intercalated and exfoliated clay–polymer composites can be produced using suitable methods.[18] It is required to use nanoscale clays to achieve intercalated or exfoliated composites.[16,17] The resulting composites are known as nanocomposite materials. Among these materials, nanocomposite hydrogels are a class of nanocomposite polymers as they can be synthesized through insertion of water soluble polymers into layered nanoclays through polymerization of hydrophilic monomers in the presence of layered nanoclays. Because of its low cost and unique characteristic such as good water adsorption, extensive swelling in water, and cation exchange capacity, sodium montmorillonite (Na-MMt) as inorganic layered clay is the interest of researchers.[19,20]

Synthesis and swelling behavior of hydrogels containing 2-acrylamido-2-methylpropane sulfonic acid (AMPS) have been investigated.[21–25] Also, because of their biocompatibility, biodegradability, and nontoxicity, polysaccharides[26–28] and proteins[29–31]

Correspondence to: G. Bagheri Marandi (marandi@kiau.ac.ir).

have been used to synthesize biopolymer-based superabsorbents or nanocomposite hydrogels. In the present study, we attempted to synthesize a novel collagen-based superabsorbent nanocomposite using the acrylamide (AAm) and AMPS monomers a well as Na-MMt clay, and investigated the effect of reaction variables on the equilibrium swelling (ES) capacity. The aim of using AMPS as monomer was to produce anionic superabsorbent with high swelling capacity. The swelling ratio in various salt solutions was also determined and additionally, the swelling of the hydrogels was measured in solutions with pH ranged 1–13. Water retention capacity (WRC) under heating was also measured.

EXPERIMENTAL

Materials

Hydrolyzed collagen (Parvar Novin-E Tehran Co., M_w = 2000–20000 Da) was industrial grade, which is available in the market and has insoluble phosphate salts. To determine the amount of these salts, three samples (each sample 2.0 g) were examined for determination of these insoluble materials. After dissolving industrial collagen in water, it was filtered and the remaining insoluble salts dried at 50°C to constant weight. The content of insoluble salts was determined to be 25% ± 1%.[31] Methylenebisacrylamide (MBA), ammonium persulfate (APS), AAm, and AMPS were from Merck Co., Germany. Natural Na-MMt (sodium Cloisite) as a clay with cation exchange capacity of 92 mequiv./100 g of clay was provided by Southern Clay Products. Ninety volume percent of its dry powder has particle size less than 13 μm, according to the manufacturer's information. Double distilled water was used for the hydrogel composite preparation and swelling measurements. All other ingredients were analytical grades and were used as received.

Preparation of the hydrogel nanocomposite

Variable amounts of the clay particles (0.2–0.7 g) were added to a two-neck reactor equipped with a magnetic stirrer, including 50 mL distilled water. The suspension solution was stirred for 24 h at room temperature. Then, the reactor was immersed in a water bath preset at a desired temperature (80°C) and then purified hydrolyzed collagen (1.0 g), the crosslinker solution (0.05–0.18 g MBA in 5 mL H_2O), certain weight ratio of AMPS/AAm [≈ 4% (0.16 g/3.84 g) to ≈ 40% (1.2 g/2.8 g)] in 10 mL H_2O, were added to the reaction mixture, respectively. After stirring for 1 h, the initiator solution (0.02–0.14 g APS in 5 mL H_2O) was added to the mixture. After the completion of the reaction (60 min), the produced hydrogel nanocomposite was poured into excess nonsolvent ethanol (200 mL) and retained for 2 h to dewater, and then the product was filtered and washed with 200 mL fresh ethanol. The filtered composite was dried in an oven at 60°C for 7 h. After grinding, the powdered composite was stored away from moisture.

Measurement of gel content

To determine the gel content values, 0.05 g of dried sample was dispersed in double distilled water to swell for 72 h. After filtration, the extracted gel was dewatered by ethanol, dried for 5 h at 70°C, and then reweighed. Gel content (gel %) was calculated by eq. (1).

$$\text{Gel } \% = (M/m) \times 100 \tag{1}$$

where, M and m stand for final and initial weight of sample, respectively.

Swelling measurements

A tea bag (i.e., a 100 mesh nylon screen) containing an accurately weighted powder sample (0.05 ± 0.001 g) was immersed entirely in 250 mL distilled water and allowed to soak for 2 h at room temperature. The sample particle sizes were 40–60 mesh. The tea bag was hung up for 15 min to remove excess water. The ES was calculated by the following equation:

$$\text{ES (g/g)} = \frac{\text{weight of swollen} - \text{weight of dried gel}}{\text{weight of dried gel}} \tag{2}$$

The accuracy of the measurements was ± 3%. Swelling measurements of hydrogels in salt solutions and various pHs was according to distilled water.

Absorbency at various pHs

Individual solutions with acidic and basic pHs were prepared by dilution of HCl (pH 1.0) and NaOH (pH 13.0) solutions, respectively. The pH values were precisely checked by a pH-meter (Metrohm/827, accuracy ± 0.1). Then 0.05 ± 0.001 g of the dried sample was used for the swelling measurements, according to eq. (2). The pH-sensitivity of the optimized sample was investigated in terms of swelling and deswelling of the final product at two basic (pH 8.0) and acidic (pH 2.0) solutions, respectively. The swelling capacity of the hydrogels at each pH was measured according to eq. (2) at consecutive time intervals. In these experiments, for each cycle, a fresh solution was used.

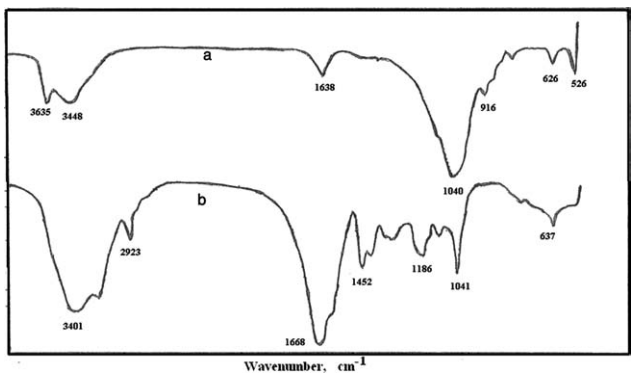

Figure 1 FTIR of (a) pristine clay and (b) nanocomposite hydrogel.

Swelling kinetics

To study the rate of absorbency of the synthesized nanocomposite hydrogels, approximately (0.05 ± 0.001 g) with various particle sizes were poured into weighted tea bags and immersed in 250 mL distilled water. The water absorbency was measured as a function of time.

Instrumental analysis

Optimized hydrogel nanocomposite was used to study XRD, scanning electron microscopy (SEM), and FTIR. So, after purifying nanocomposite hydrogel according to measurement of gel content, the dried powders were used to study instrumental analysis. Dried nanocomposite was coated with a thin layer of gold and imaged in a SEM instrument (Philips, XL30). One-dimensional, wide angle X-ray diffraction patterns were obtained by using a Philips X'Pert MPD X-ray diffractometer with wavelength, $\lambda = 1.54$ Å (Cu-Kα), at a tube voltage of 40 KV and tube current of 40 mA. FTIR spectra of samples were taken in KBr pellets using an Perkin–Elmer PE 1600 FTIR spectrophotometer.

RESULTS AND DISCUSSIONS

Synthesis and characterization

The nanocomposite superabsorbents were prepared by simultaneous graft copolymerization of AMPS and AAm onto collagen backbones in the presence MBA and Na-MMt as crosslinker and clay, respectively. APS was used as initiator. The mechanism of grafting can be assumed similar to our previous work.[31] It may be noted that not only grafting of monomers can take place, but also crosslinked copolymer can be formed. These crosslinked copolymers will capture inside hydrogels.

The FT-IR spectroscopy was carried out to confirm the chemical structure of the hydrogel nanocomposite. Figure 1(a,b) shows the spectra of the nanoclay and nanocomposite superabsorbent, respectively. In Figure 1(a), the characteristic vibration bands of the nanoclay (—OH stretch from lattice hydroxyl, —OH stretch from free H_2O, —OH bending, and Si—O stretch) are shown at 3635, 3448, 1639, and 1040 cm^{-1}, respectively. In the spectrum of the nanocomposite [Fig. 1(b)], the characteristic band at 1668 cm^{-1} can be attributed to C=O stretching in the carboxamide functional groups, absorption bands at 1041 and 1186 cm^{-1} attributed to S=O stretching in sulfonic acid functional group. In addition, by comparing with Figure 1(a), the absorption peaks at 3635 and 3448 cm^{-1} attributed to the OH groups, and intense band at 1040 cm^{-1}, attributed to the Si—O stretching on the nanoclay, disappeared after reaction. Therefore, it can be suggested that the strong chemical interaction takes place between the Si—O and —OH groups of the nanoclay particles with functional groups of AMPS and AAm monomers during the graft copolymerization reaction.

The XRD patterns of pristine clay and nanocomposites containing 3.8, 5.6, 9, and 12 wt % of clay are shown in Figure 2. As can be seen from this figure, the XRD profile of pristine Na-MMt shows a diffractive peak at $2\theta = 7.6$, corresponding to the distance of clay sheets with d spacing 11.61 nm [Fig. 2(a)].

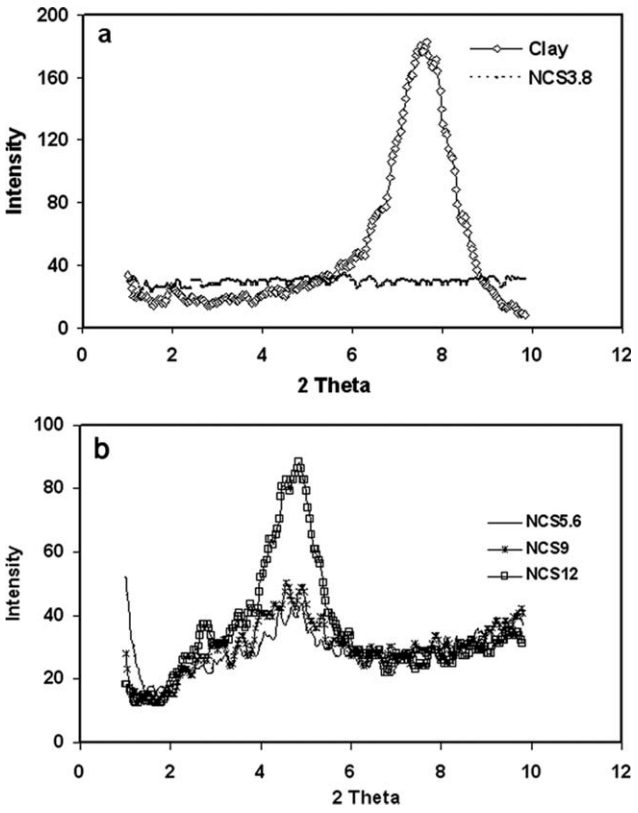

Figure 2 XRD patterns of (a) pristine Na-MMt and nanocomposite superabsorbent (NCS) containing 3.8 wt % of clay, (b) 5.6, 9, and 12 wt % of clay, respectively.

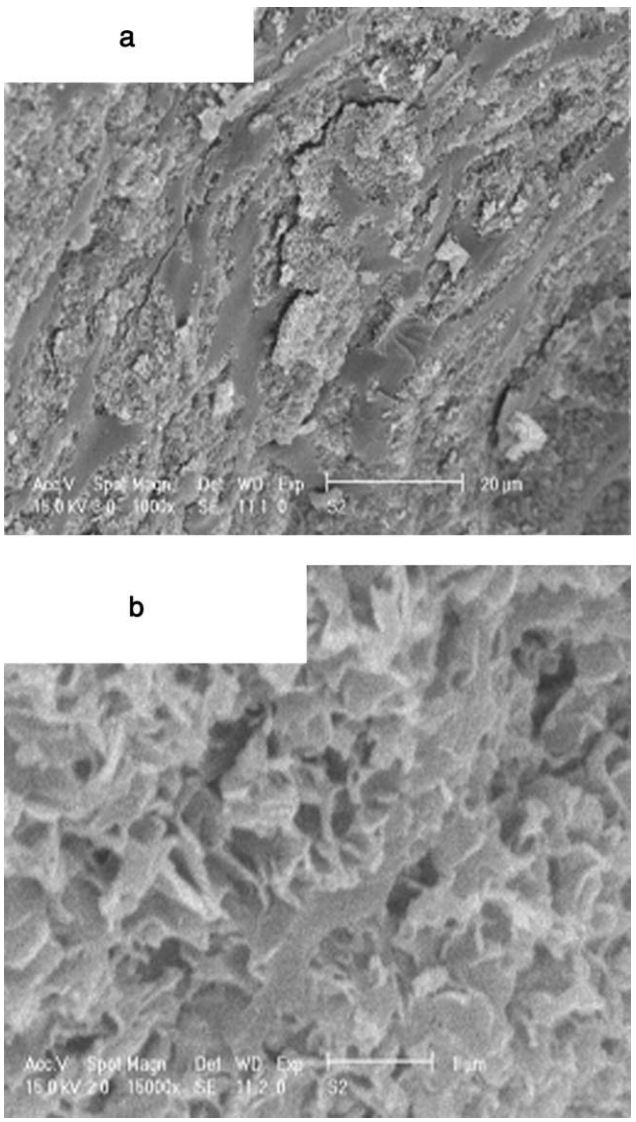

Figure 3 SEM micrographs of nanocomposite hydrogel with (a) scale bar of 20 μm and (b) scale bar of 1 μm.

Stirring of clay for 24 h subsequently *in situ* polymerization of AAm and AMPS in the presence of MBA crosslinker leads to a nanocomposite hydrogel, and the XRD profile of these nanocomposites is shown in Figure 2(a,b). The results showed that the clay content affects its dispersion type in nanocomposite. It was observed that there is no diffraction peak in nanocomposites containing 3.8 wt % of clay, and it can be concluded that the clay layers are completely exfoliated and uniformly dispersed in organic network [Fig. 2(a)]. However, when the clay content is higher than 3.8 wt %, the XRD patterns of nanocomposites showed a peak at $2\theta = 4.67$, 4.6, and 4.7 for nanocomposites containing 5.6, 9, and 12, respectively, [Fig. 2(b)]. This observation suggests that the clay is not in exfoliated form and exists in intercalated structure.

One of the most important properties of nanocomposites that can be considered is hydrogel microstructure morphology. Figure 3(a,b) shows the surface morphology of optimized nanocomposite hydrogels with 20 and 1 μm of scale bars, respectively. According to this image, nanocomposite hydrogel contains a porous structure.

Effect of nanoclay content on swelling

The swelling capacity of nanocomposite in deionized water as a function of nanoclay content was studied by varying the nanoclay amount from 3.8 to 12 wt % (Fig. 4). Maximum swelling (681 g/g) was obtained at 5.6 wt % of nanoclay. It is observed that the absorbency is substantially increased from 441 g/g for free-clay superabsorbent to 681 g/g for optimum clay content and then decreased. When the Na-MMt content in superabsorbent nanocomposite is low, the ionization of Na-MMt takes place easily, and subsequently the osmotic pressure on the inside of the nanocomposite is increased. Enhancement of osmotic pressure in hydrogel causes an increase in water absorbency of hydrogel.[32,33] However, the swelling-loss after the maximum may be originated from decrease in ionization of Na-MMt and subsequent decrease in osmotic pressure. On the other hand, when the content of clay is higher than 5.6 wt %, clay counterions remain in the local volume around the clay particles or between the plates and do not contribute to the total osmotic pressure inside the hydrogel.[34] Also, it has been reported that MMt can act as crosslinker in hydrogel systems. It is clear that by increasing MMt content, crosslinking points increase and results in low swelling capacity.[35,36] The effect of clay amount on the gel content was shown in this figure. According to results, it was observed that with increasing clay amount in superabsorbent composition, the gel content is increased.

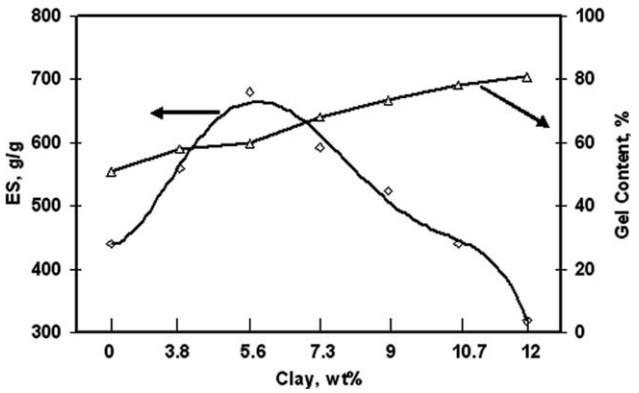

Figure 4 Effect of nanoclay on the water absorbency and gel content. Reaction conditions: collagen 1.0 g, MBA 0.006 mol/L, weight ratio of AMPS/AAm 19%, APS 0.005 mol/L, 80°C, 60 min.

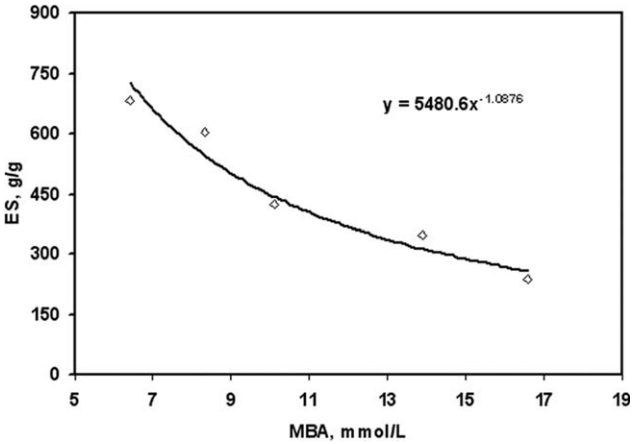

Figure 5 Effect of crosslinking concentration on water absorbency of hydrogel. Reaction conditions: collagen 1.0 g, weight ratio of AMPS/AAm 19%, APS 0.005 mol/L, nanoclay 0.3 g, 80°C, 60 min.

This observation can be attributed to the interaction between clay and soluble part of synthesized hydrogel. In fact, the increase in gel content with increasing clay content may be because clay acts as a crosslinker. A similar observation has been reported by Kokabi et al.[37] in poly (vinyl alcohol) nanocomposites hydrogels using Na-MMt clay.

Effect of MBA concentration on swelling

Figure 5 demonstrates the effect of crosslinker concentration on the swelling capacity of the collagen-*g*-poly(AMPS-*co*-AAm)/nanoclay hydrogel nanocomposite. As shown in this figure, greater absorbency (681 g/g) is obtained at 0.006 mol/L of crosslinker. In fact, the free space between the copolymer chains decreases at high concentration of MBA, and consequently the highly crosslinked rigid structure can not be expanded to hold a large quantity of water. It may be noted that the hydrogels prepared with MBA concentration lower than 0.006 mol/L did not posses good dimensional stability. Therefore, the strength of the swollen gel was not sufficient to refer the hydrogels as "real superabsorbent."

The following power law relationship between ES capacity and MBA concentration [eq. (3)] was deduced from Figure 5.[38]

$$\mathrm{ES} = K\,[\mathrm{MBA}]^{-n} \tag{3}$$

where K and n in eq. (3) are constant for an individual superabsorbent. The n value represents the sensitivity of the hydrogel to the crosslinker content, whereas the K value gives a useful criterion for comparing the extent of swelling at a fixed crosslinker content (i.e., the higher the K value, the higher the ES capacity). The values $K = 5480$ and $n = 1.1$ were obtained from the curve fitted with eq. (3).

Effect of monomers ratio on swelling capacity

Different hydrogels with various AMPS/AAm weight ratios were synthesized through changes in amounts of AMPS (0.16–1.2 g) and AAm (3.84–2.8 g). The swelling capacity of the hydrogels, prepared with various ratios of monomers, is shown in Figure 6. It is observed that the absorbency is substantially increased with an increase in the AMPS/AAm ratio and then decreased. The initial increment in swelling values can be attributed to increase in ionic groups existing in copolymer chains along with increase of AMPS in the hydrogel, which allows polymer coils to expand more easily. The swelling loss after the maximum may be originated from reducing the hydrogel strength and increasing sol content because of the higher amount of AMPS.[39] As shown in Figure 6, an AMPS/AAm ratio of 19% provides the best values of swelling.

Effect of APS concentration on swelling

The relationship between initiator concentration and water absorbency values was studied by varying the APS concentration from 0.001 to 0.009 mol/L (Fig. 7). Maximum swelling (681 g/g) was obtained at an initiator concentration of 0.005 mol/L. More or less than this concentration gives a hydrogel with decreased swelling capacity. The number of active free radicals on the collagen backbone decreased at lower concentrations than 0.005 mol/L. Initial increment in water absorbency attributed to increased number of active free radicals on the protein backbone. The subsequent swelling loss can be explained as follows: (a) an increase in termination reaction by bimolecular collisions, which was referred to as self-crosslinking (the greater number of free radicals on the collagen backbone causes more bond formation

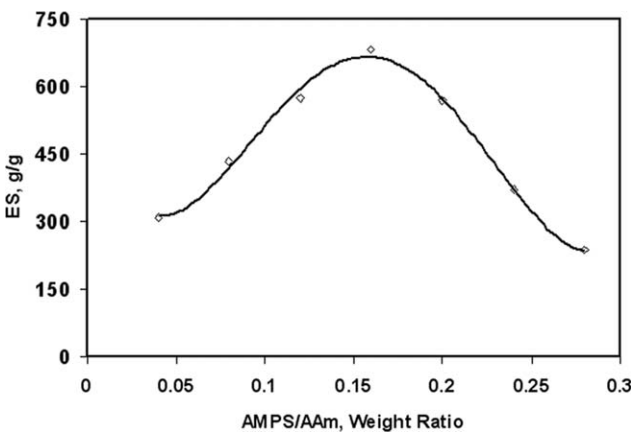

Figure 6 Effect of weight ratio of AMPS/AAm on the water absorbency. Reaction conditions: collagen 1.0 g, MBA 0.006 mol/L, APS 0.005 mol/L, nanoclay 0.3 g, 80°C, 60 min.

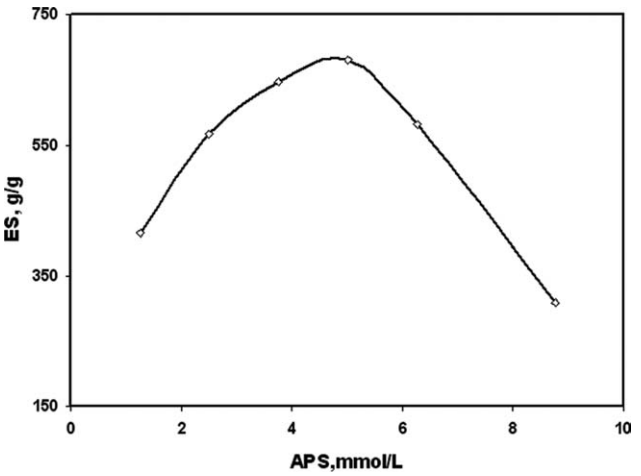

Figure 7 Effect of initiator concentration on the water absorbency. Reaction conditions: collagen 1.0 g, MBA 0.006 mol/L, weight ratio of AMPS/AAm 19%, nanoclay 0.3 g, 80°C, 60 min.

at various sites of the polymeric chains),[40] (b) the free radical degradation of collagen backbones by sulfate radical anions is an additional reason for swelling loss at higher APS concentration, and (c) the decrease in molecular weight (M_w) of the grafted polymer produces a lower swelling value. The latter can be explained by the inverse relationship between M_w and initiator concentration.

Swelling kinetics

A preliminary study was conducted on superabsorbent swelling kinetic. Figure 8 represents the dynamic swelling behavior of the optimally prepared collagen-*g*-poly(AMPS-Co-AAm)/nanoclay hydrogel with various particle sizes in distilled water. Initially, the rate of water uptake increases sharply and then begins to level off. A power law relationship is obvious from Figure 8. The data may be well fitted with a Voigt- based equation[38]:

$$S_t = S_e\ (1 - e^{t/\tau}) \tag{4}$$

where S_t (g/g) is swelling at time t, S_e is the ES (power parameter, g/g), t is time (min) for swelling to an extent S_t, and τ (min) stands for the "rate parameter." The rate parameter is a measure of the swelling rate (i.e., the lower the τ value, the higher the rate of swelling). The rate parameters were found to be 0.86, 1.44, 1.72 min for the nanocomposites with particle sizes of 100–250, 250–400, and 400–550 μm, respectively. It is well-known that the swelling kinetic for the hydrogels is significantly influenced by the particle size of the absorbents. With a lower particle size, a higher rate of water uptake is observed. An increase in the rate of absorption would be expected from the increase in surface area with decreasing particle size of hydrogel composite. In comparison to our previous work,[31] the τ values for collagen-*g*-poly(acrylic acid-*co*-sodium acrylate) hydrogel was variable from 3.2 to 6.4 min. Although the content of nonionic AAm monomer is high in nanocomposite hydrogel, the rate of swelling is higher than anionic collagen-*g*-poly(acrylic acid-*co*-sodium acrylate) hydrogel. This high rate of swelling can be attributed to the highly porous structure of nanocomposite and presence of Na-MMt clay.

In general, the rate of absorption and the ultimate degree of absorption increased as the particle size became smaller. These effects are attributed to an increase in the surface area of absorbent accessible to the water. The increase in rate of absorption is attributed to more water absorbed for a given depth of permeation into the absorbent particles, and an increase in the ultimate degree of absorption is attributed to more water being held in the volume between the particles.[41]

Swelling in various salt solutions

It is important to know the swelling behavior of hydrogels in salt solution for many applications, especially agricultural and horticultural ones. It is well known that water absorbency decreases with increasing ionic strength of salt solutions. This result may be attributed to the reduction in the osmotic pressure difference between the hydrogel and the external salt solution with increasing ionic strength. Also, the screening effect of the additional cations on the anionic groups causes a nonperfect anion–anion electrostatic repulsion and reduces water absorbency.[42] In addition, ionic crosslinking of the hydrogel in the multivalent cation solution is another cause for reduction of water absorbency. Figure 9 shows the effect of the ionic strength of various chloride salt solutions on the water absorbency

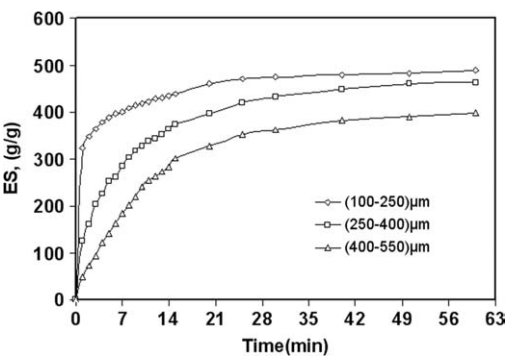

Figure 8 Representative swelling kinetics of the optimized hydrogel composite with various particle sizes in distilled water.

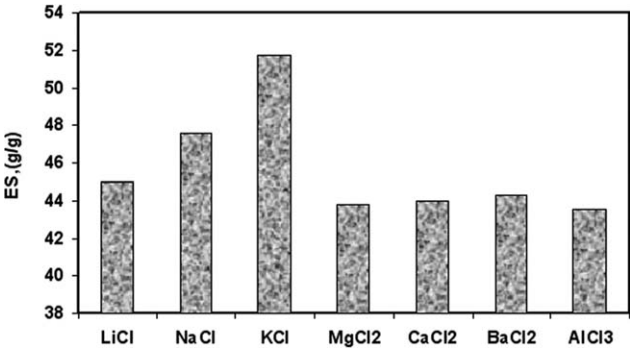

Figure 9 Swelling capacity of the optimized hydrogel composite in various salt solutions with the same concentrations (0.15 mol/L).

of the hydrogels. The water absorbency decreases with increasing ionic strength of salt solutions. It is apparent that the swelling decrease is strongly dependent on the charge and radius of the cation added to the swelling medium. With increasing the charge of cation, degree of crosslinking increased and swelling is consequently decreased.

Therefore, the absorbency for the optimized hydrogel in the studied salt solution is in the order of monovalent > divalent > trivalent cations. As a result, the absorbency in salt solutions is in the order of $K^+ > Na^+ > Li^+$ and $Ba^{2+} > Ca^{2+} > Mg^{2+}$ and $> Al^{3+}$, respectively. The results show that the swelling in salt solution with di- and trivalent cations for this hydrogel containing sulfonic groups is higher than hydrogels containing carboxylate groups. In the our previous work, the water absorbency of collagen-*g*-poly(acrylic acid) hydrogel in Ca^{2+} solution was achieved at $\sim$ 8 g/g,[31] but it was obtained at $\sim$ 44 g/g for nanocomposite hydrogels containing sulfonic groups. It may be attributed to high interaction of multivalent cation with carboxylate groups.

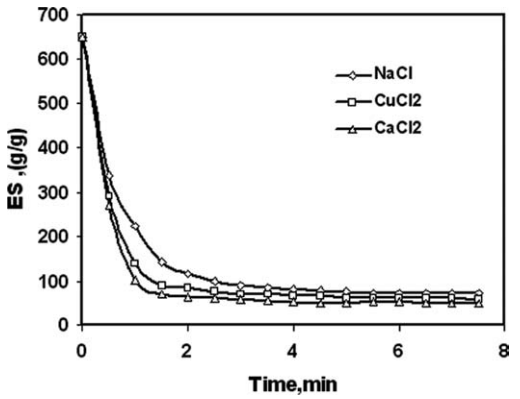

Figure 10 Kinetics of dewatering swollen hydrogel in various salt solutions with the same concentrations (0.15 mol/L).

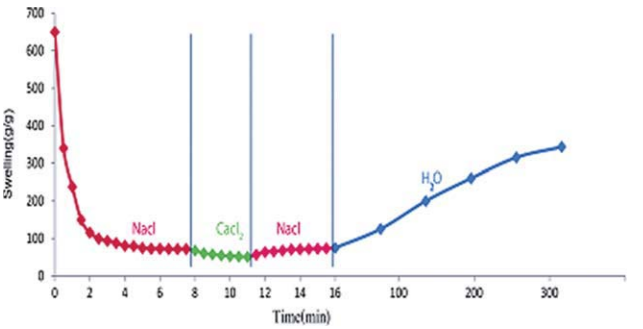

Figure 11 Water lost and water uptake of swollen hydrogel in aqueous media. [Color figure can be viewed in the online issue, which is available at wileyonlinelibrary.com.]

Kinetics of dewatering swollen hydrogel in different chloride salt solutions

Figure 10 illustrates the relationship between type of salt solution and water lost of swollen hydrogel. It is observed that the water lost slope increases with increasing in the charge of cation. Degree of crosslinking increases with increasing the charge of cation, and swelling is consequently decreased. Also, Ca^{2+} ions, have a bigger cationic radius than the Cu^{2+} ion; therefore, the degree of crosslinking with sulfonic and amide functional groups is more than that of the Cu^{2+} ion.

Figure 11 demonstrates the salt solution-dependent swelling reversibility of the hydrogel. This figure shows the reversible swelling–deswelling behavior of the hydrogel composite in various solutions. Water lost is strongly dependent on the type of salt solutions. In the $CaCl_2$ solution may be formed a reversible complex between Ca^{2+} ion with sulfonic and amide groups. So, when the hydrogel transfer to NaCl solution and then distilled water, the water absorbency of the hydrogel increased.

Figure 12 presents the dynamic dewatering behavior of the optimized hydrogel with various particle sizes in NaCl solution. Initially, the rate of water lost

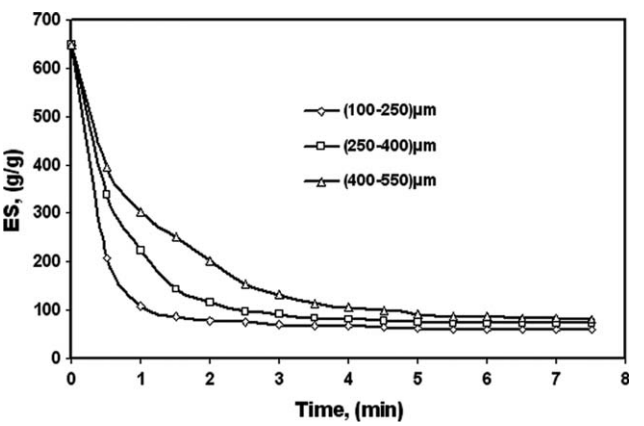

Figure 12 Kinetics of dewatering of the swollen hydrogel with different particle sizes in NaCl solution.

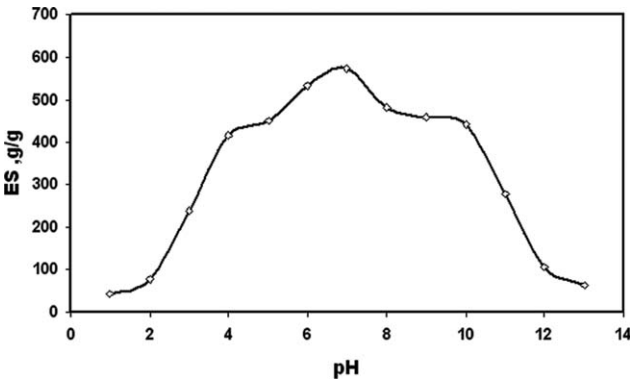

Figure 13 Effect of pH of solutions on the swelling capacity of the optimized hydrogel composite.

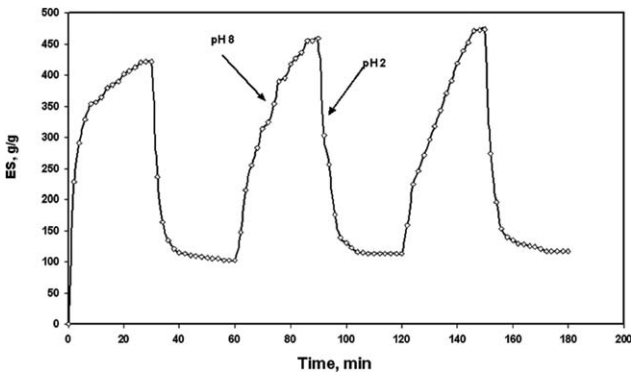

Figure 14 On–off switching behavior as reversible pulsatile swelling (pH 8.0) and deswelling (pH 2.0) of the optimized hydrogel composite.

is sharp and then begins to level off. It is well-known that the dewatering kinetic for the hydrogel is significantly influenced by the particle size of the absorbent. With a lower the particle size, a higher rate of water lost is observed. An increase in the rate of the water lost would be expected from the increase in surface area with decreasing particle size of hydrogel composite.

pH-dependent swelling of the hydrogel

To investigate the sensitivity of the hydrogel to pH, firstly the ES of the hydrogel was studied at various pHs, ranging from 1.0 to 13.0 (Fig. 13). Because the swelling capacity of the hydrogel is appreciably reduced by the addition of counter ions to the swelling medium, no buffer solutions were used. Therefore, stock NaOH (pH 13.0) and HCl (pH 1.0) solutions were diluted with distilled water to reach desired basic and acidic pHs, respectively. Nonionic amide and ionic sulfonate groups exist in nanocomposite hydrogel. It has been reported that hydrogels containing sulfonate groups exhibit pH-independent swelling behavior.[23] In fact, all sulfonate groups dissociate completely in the overall pH range (the pK_a of methanesulfonic acid is -1.86[43]). But, this pH-independent behavior can be observed by using buffer solution with same concentration and ionic strength. As mentioned above, in the present work, we prepared solutions with various pHs using dilution method. So, the ionic strength of the solutions will not be the same.

According to Figure 13, the absorbency of the optimized hydrogel increased as the pH increased from 1.0 to 7.0 and then decreased in pH higher than 7.0. Maximum swelling (575 g/g) was obtained at pH 7.0. In the pH region from 1 to 2, two factors affect low swelling of hydrogel: firs, the screening effect of H^+ ions causing a nonperfect anion–anion electrostatic repulsion, and also the presence of high concentration of H^+, which causes H^+ counterions to remain around sulfonate groups and limit complete dissociation of sulfonic acid groups.[44] The swelling ratio increased rapidly as the pH of the solutions was increased from 2 to 7. With increasing the pH, the sulfonic acid groups were gradually ionized, and the electrostatic repulsion between $-SO_3^-$ groups caused an enhancement of the swelling capacity. A charge screening effect of excess Na^+ in the swelling media, which shielded the sulfonate anions and prevented effective anion–anion repulsion, was the reason for the swelling loss in the basic solutions (pH $>$ 7). Similar observation has been reported by Atta.[24]

Because these hydrogel composites showed different swelling behaviors in various pH solutions, we investigated the pH reversibility of these hydrogels in 0.01*M* solutions with pH 2 and pH 8 (Fig. 14). Since the pH of the working solutions may be changed by protonation–deprotonation process of hydrogel, a fresh solution was used in each cycle. At pH 8, the hydrogel swelled up to 421 g/g because of anion–anion repulsive electrostatic forces, whereas at pH 2.0, it shrank within a few minutes because of protonation of the sulfonate groups. Because ofthe

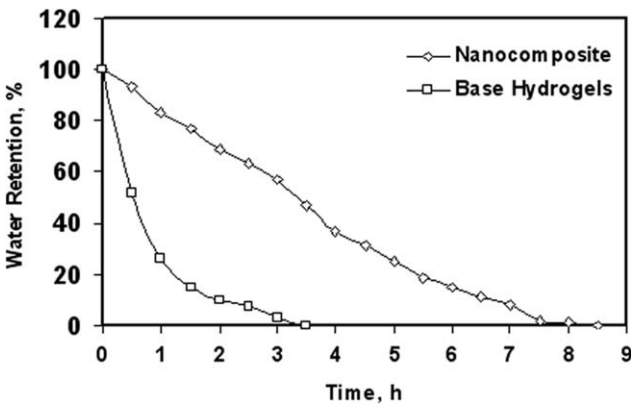

Figure 15 Thermal stability of optimized composite and the normal hydrogel, swollen in distilled water.

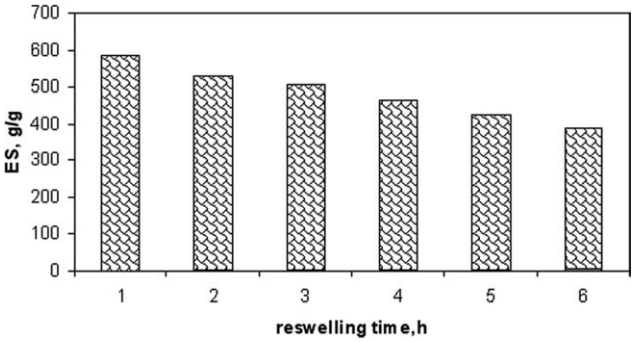

Figure 16 Reswelling capacity of optimized composite.

using the fresh solutions, as show in Figure 14, the absorbency was increased after each cycle.

Water retention capacity

It is important to investigate the thermal stability of a hydrogel composite in view of practical application. Figure 15 shows the WRC of the swollen composite and the synthesized hydrogel under same condition with composite but without any nanoclay at 60°C. According to the literature, the water in a hydrogel can be classified into bound water, half-bound water, and free water. Compared to bound water and half-bound water, the free water in a hydrogel has high mobility and can easily be lost. The percentages of bound water and half-bound water content in swollen gel are related to the number of hydrophilic groups (—SO_3^-, —SO_3H, —$CONH_2$ and —OH) in a unit volume in hydrogel. As shown in Figure 15, after 3.5 h, while nanocomposite hydrogel keep 57 wt % of absorbed water, the hydrogel without clay losses its absorbed water completely. This observation shows good WRC for nanocomposite.

Figure 16 indicates reswelling capacity of the optimized composite at 100°C. After that the swollen hydrogel thoroughly loses its absorbed water under heating, the resulting dry sample still retains a good water absorbing ability. According to Figure 16, the sample still retains $\sim$ 60% of its initial water absorbency even after repeating the swelling–reswelling-swelling test six times at 100°C.

CONCLUSIONS

Synthesis of superabsorbent nanocomposite was done by using nanoclay particles in aqueous media at 80°C under normal atmospheric conditions. Main conclusions may be summarized as follows:

- The optimum reaction conditions to obtain improved water absorbency (681 g/g) were found to be: purified hydrolyzed collagen 1.0 g, MBA 0.006 mol/L, weight ratio of AMPS/AAm 19%, APS 0.005 mol/L, and nanoclay 0.3 g.
- XRD patterns showed that content of clay in nanocomposite composition can affect its type of dispersion in nanocomposite structure. Although for 3.8 wt % of clay an exfoliated nanocomposite was achieved, higher than this content result in intercalated dispersion of clay in nanocomposite.
- SEM micrograph of optimized nanocomposite showed a highly porous structure. This porosity caused high rate of swelling for nanocomposite with τ values of 0.86, 1.44, 1.72 min for the nanocomposites with particle sizes of 100–250, 250–400 and 400–550 μm, respectively,.
- High swelling capacity was achieved for nanocomposite in $CaCl_2$ solution (44 g/g). This high swelling capacity can be attributed to presence of sulfonic groups in nanocomposite composition.
- pH-Dependent swelling of nanocomposite was obtained by varying pH of swelling media.
- On heating of swollen nanocomposite and free-clay hydrogel, it was observed that nanocomposite keeps 57 wt % of absorbed water, but hydrogel without clay losses its absorbed water completely. This observation shows good WRC for nanocomposite.

References

1. Dimitrov, M.; Lambov, N.; Shenkov, S.; Dosseva, V.; Baranovski, V. Acta Pharm 2003, 53, 25.
2. Eshel, H.; Dahan, L.; Dotan, A.; Dodiuk, H.; Kenig, S. Polym Bull 2008, 61, 257.
3. Aoki, T.; Kawashima, M.; Katono, H.; Sanui, K.; Ogata, N.; Okano, T.; Sakurai, Y. 1994, 27, 947.
4. Hu, Y.; Horie, K.; Tori, T.; Ushiki, H.; Tang, X.C. Polym J 1993, 25, 123.
5. Hirokawa, Y.; Tanaka, T. J Chem Phys 1984, 81, 6379.
6. Murali, M. Y.; Keshava, M. P. S.; Mohana, R. K. React Funct Polym 2005, 63, 11.
7. Mohana, R. K.; Padmanabha, R. M.; Murali, M. Y. Polym Int 2003, 52, 768.
8. Rudzinski, W. E.; Dave, A. M.; Vaishnav, U. H.; Kumbar, S. G.; Kulkarni, A. R.; Aminabhavi, T. M. Des Monomers Polym 2002, 5, 39.
9. Bajpai, A. K.; Giri, A. React Funct Polym 2002, 53, 125.
10. Mahdavinia, G. R.; Mousavi, S. B.; Karimi, F.; Marandi, G. B.; Garabaghi, H.; Shahabvand, S. Express Polym Lett 2009, 3, 279.
11. Darvari, R.; Hasirci, V. J Microencapsul 1996, 13, 9.
12. Wang, W.; Wang, A. Carbohydr Polym 2009, 77, 891.
13. Qi, X.; Liu, M.; Chen, Z.; Liang, R. Polym Adv Technol 2007, 18, 184.
14. Bagheri Marandi, G.; Hosseinzadeh, H. Polym Polym Compos 2007, 15, 395.
15. Wan, T.; Wang, W.; Yuan, Y.; He, W. J Appl Polym Sci 2006, 102, 2875.
16. Jordan, J.; Jacob, K. I.; Tannenbaum, R.; Sharaf, M. A.; Jasiuk, I. Mater Sci Eng 2005, 393, 1.

17. Goettler, L. A.; Lee, K. Y.; Thakkar, H. Polym Rev 2007, 47, 291.
18. Giannelis, E. P.; Krishnamoorti, R.; Manias, E. Adv Polym Sci 1999, 138, 108.
19. Sun, L.; Boo, W. J.; Liu, J.; Tien, C. W.; Sue, H. J.; Marks, M. J.; Pham, H. Polym Eng Sci 2007, 47, 1708.
20. Paranhos, C. M.; Soares, B. G.; Machado, J. C.; Windmoller, D.; Pessan, L. A. Eur Polym J 2007, 43, 4882.
21. Abdel-Azim, A. A.; Farahat, M. S.; Atta, A. M.; Abdel-Fattah, A. A. Polym Adv Technol 1998, 9, 282.
22. Okay, O.; Sariisik, S. B.; Zor, S. D. J Appl Polym Sci 1998, 70, 567.
23. Durmaz, S.; Okay, O. Polymer 2000, 41, 3693.
24. Atta, A. M. Polym Adv Technol 2002, 13, 567.
25. Liu, Y.; Xie, J. J.; Zhang, X. Y. J Appl Polym Sci 2003, 90, 3481.
26. Zeppa, C.; Gouanve, F.; Espuche, E. J Appl Polym Sci 2009, 112, 2044.
27. Lu, J.; Wang, A. J Appl Polym Sci 2008, 110, 678.
28. Wang, W.; Zheng, Y.; Wang, A. Polym Adv Technol 2008, 19, 1852.
29. Lai, J.; Fang, R.; Wang, L.; Tu, K.; Zhao, C.; Qian, X.; Zhan, S. J Appl Polym Sci 2009, 113, 3944.
30. Yu, L.; Gu, L. Polym Int 2009, 58, 66.
31. Bagheri Marandi, G.; Hariri, S.; Mahdavinia, G. R. Polym Int 2009, 58, 227.
32. Li, A.; Zhang, J.; Wang, A. J Appl Polym Sci 2007, 103, 37.
33. Xia, X.; Yih, J.; D, Souza, N. A.; Hu, Z. Polymer 2003, 44, 3389.
34. Alaie, J; Vashegani-Farahani, E.; Rajmatpour, A.; Semsarzadeh, M. A. Eur Polym J 2008, 44, 2024.
35. Xu, K.; Wang, J.; Xiang, S.; Chen, Q.; Zhang, W.; Wang, P. Appl Clay Sci 2007, 38, 139.
36. Haragachi, K.; Takehisa, T. Adv Mater 2002, 14, 1120.
37. Kokabi, M.; Sirousazar, M.; Mohammad-Hasan, Z. Eur Polym Mater 2007, 43, 773.
38. Omidian, H.; Hashemi, S. A.; Sammes, P. G.; Meldrum, I. Polymer 1998, 39, 6697.
39. Gad, Y. H. Radiat Phys Chem 2008, 77, 1101.
40. Liu, M.; Liang, R.; Zhan, F.; Liu, Z.; Niu, A. Polym Int 2007, 56, 729.
41. Bagheri Marandi, G.; Esfandiari, K.; Biranvand, F.; Babapour, M.; Sadeh, S.; Mahdavinia, G. R. J Appl Polym Sci 2008, 109, 1083.
42. Lee, W. F.; Wu, R. J. J Appl Polym Sci 1996, 62, 1099.
43. Serjaent, E. P.; Dempsey, B. IUPAC Chemical Data Series 23; Pergamon Press: New York, 1979.
44. Rosa, F.; Bordado, J.; Casquilho, M. J Polym Sci Part B: Polym Phys 2004, 42, 505.